

Purification and Characterization of the Low Molecular Weight Protein Tyrosine Phosphatase, Stp1, from the Fission Yeast *Schizosaccharomyces pombe*[†]

Zhong-Yin Zhang,^{*,‡} Gaochao Zhou,[§] John M. Denu,[§] Li Wu,[‡] Xuejun Tang,^{||} Odile Mondesert,[⊥] Paul Russell,[⊥] Elizabeth Butch,[§] and Kun-Liang Guan[§]

Departments of Molecular Pharmacology and Biochemistry, Albert Einstein College of Medicine, 1300 Morris Park Avenue, Bronx, New York 10461, Department of Biological Chemistry, University of Michigan, Ann Arbor, Michigan 48109, and Departments of Molecular and Cell Biology MB-3, The Scripps Research Institute, La Jolla, California 92037

Received April 20, 1995; Revised Manuscript Received June 6, 1995[®]

ABSTRACT: Genetic screening in fission yeast has identified a gene named *stp1*⁺ that rescues *cdc25-22* [Mondesert et al. (1994) *J. Biol. Chem.* 269, 27996–27999]. This gene encodes a 17.4 kDa protein that is 42% identical to members of the low molecular weight protein tyrosine phosphatases (low *M_r* PTPases) previously known to exist only in mammalian species. A simple and efficient purification procedure was developed to obtain the homogeneous recombinant yeast low *M_r* PTPase, Stp1, in large quantities suitable for kinetic and structural studies. Authentic Stp1 was produced as judged by amino terminal protein sequencing and electrospray ionization mass spectrometry analyses. Stp1 was shown to possess intrinsic phosphatase activity toward both aryl phosphates (such as phosphotyrosine) and alkyl phosphates (such as phosphoserine). Stp1 also dephosphorylated phosphotyrosyl peptide/protein substrates. The yeast enzyme was 6-fold slower than the mammalian enzymes, which made it amenable to pre-steady-state stopped-flow spectroscopic kinetic analysis at 30 °C and pH 6.0. Burst kinetics was observed with Stp1 using *p*-nitrophenyl phosphate as a substrate, suggesting that the rate-limiting step corresponds to the decomposition of the phosphoenzyme intermediate. Interestingly, the bovine heart low *M_r* PTPase was capable of removing phosphate groups from both phosphotyrosyl and phosphoseryl/threonyl protein substrates with comparable efficiencies. The low *M_r* PTPases, like the Cdc25 family of phosphatases, may represent a new group of dual specificity phosphatases which may be involved in cell cycle control.

Protein phosphorylation is a fundamental post-translational modification that is involved in the regulation of numerous cell functions including cell cycle control, cell growth and differentiation, mitogenesis, metabolism, gene transcription, and the immune response. The level of protein phosphorylation on cellular proteins is tightly controlled by the concerted action of protein kinases and protein phosphatases. Low molecular weight (18 kDa) acid phosphatases (EC 3.1.3.2) are found ubiquitously in mammalian cells (Heinrikson, 1969; Chen & Chen, 1988; Zhang & Van Etten, 1990; Ramponi, 1994). These enzymes are highly specific for aryl phosphate esters and show very limited activity toward aliphatic phosphate esters, with the exception of flavin mononucleotide (FMN)¹ and certain of its structural analogs (Heinrikson, 1969; Zhang & Van Etten, 1990). They have

also been shown to hydrolyze a number of phosphotyrosine-containing peptide/protein substrates (Chernoff & Li, 1985; Waheed et al., 1988; Ramponi et al., 1989). Thus, low molecular weight acid phosphatases have been renamed as low molecular weight protein tyrosine phosphatases (low *M_r* PTPases) (Chernoff & Li, 1985; Waheed et al., 1988; Zhang & Van Etten, 1990). Although the low *M_r* PTPases are unrelated in sequence to the newly identified higher molecular weight PTPases that contain a 250-residue conserved catalytic domain (Zhang & Dixon, 1994), they do possess the PTPase signature motif (H/V)C(X)₂R(S/T) (Cirri et al., 1993; Zhang, Z.-Y., et al., 1994). Furthermore, it appears that both the low *M_r* enzymes and the rest of the PTPases utilize a common strategy to bring about phosphate monoester hydrolysis. Biochemical evidence has demonstrated that the invariant Cys and Arg residues present in the PTPase signature motif are extremely important for catalysis. Thus, the invariant Cys residue has been shown to be essential for PTPase activity and formation of a covalent phosphoenzyme intermediate (Guan & Dixon, 1991a; Wo et al., 1992; Cho et al., 1992; Cirri et al., 1993). The invariant Arg residue in the signature motif plays an important role in substrate binding and transition state stabilization (Zhang, Z.-Y., et al., 1994).

Recently, the crystal structures of the bovine low *M_r* PTPase have been solved (Su et al., 1994; Zhang, M., et al., 1994). In addition, the structures of the mammalian PTP1B (Barford et al., 1994) and the *Yersinia* PTPase (Stuckey et al., 1994) have also been determined. Although the bovine low *M_r* PTPase has distinct topologies compared with those

[†] This work was supported by a grant from NIH (DRTC 5P60 DK20541-17) to Z.-Y.Z. and a grant from the American Cancer Society (BE171) to K.-L.G.

^{*} To whom correspondence should be addressed, at the Department of Molecular Pharmacology, Albert Einstein College of Medicine, 1300 Morris Park Ave., Bronx, NY 10461. Tel: 718-430-4288; Fax: 718-829-8705.

[‡] Department of Molecular Pharmacology, Albert Einstein College of Medicine.

[§] University of Michigan.

^{||} Department of Biochemistry, Albert Einstein College of Medicine.

[⊥] The Scripps Research Institute.

[®] Abstract published in *Advance ACS Abstracts*, August 1, 1995.

¹ Abbreviations: PTPase, protein tyrosine phosphatase; Stp1, small tyrosine phosphatase; *p*NPP, *p*-nitrophenyl phosphate; FMN, flavin mononucleotide; MAP kinase, mitogen activated protein kinase; ERK, extracellular-signal regulated kinase; MBP, myelin basic protein; MEK, MAP kinase or ERK kinase; GST, glutathione *S*-transferase.

		***** *	
human(s)	1	AEQATK..SV LFVCLGNICR	SPIAEAVFRK LVWDQNISEN
human(f)	1	AEQATK..SV LFVCLGNICR	SPIAEAVFRK LVWDQNISEN
bovine	1	AEQVTK..SV LFVCLGNICR	SPIAEAVFRK LVTDQNISDN
yeast	1	MTKNIQV LFVCLGNICR	SPIAEAVFRN EVEKAGLEAR
cyanobacteria	1	MITK...L LFVCLGNICR	SPIAEGVFLH LIEQRQLTDQ
human(s)	39	W.VIDSGAVS DWNVGRSPDP	RAVSCLRNHG IHTAKHARQI
human(f)	39	W.RVDSAAITS GYEIGNPPDY	RGQSCMKRHG IPMSKVARQI
bovine	39	W.VIDSGAVS DWNVGRSPNP	RAVSCLRNHG IHTAKHARQV
yeast	38	FDTIDSCGTG AWHVGNRPDP	RTLEVLRKNG IHTKHLARKL
cyanobacteria	36	F.LVDSAGTG GWHVGNPDR	RMQAAARRRG I(65)
human(s)	78	TKEDFATFDY ILCNDESNLR	DLNRKSNQVK TCKAKIELLG
human(f)	78	TKEDFATFDY ILCNDESNLR	DLNRKSNQVK TCKAKIELLG
bovine	78	TKEDFATFDY ILCNDESNLR	DLNRKSNQVK NCRKAKIELLG
yeast	78	STSDPKNFYD IFADNDSNLR	NINRVKFPQ..GSRKVMFLG
human(s)	118	SY.DPQKQLI IEDFPYGNDS	DFETVYQQCV RCCRAFLEKA
human(f)	118	SY.DPQKQLI IEDFPYGNDS	DFETVYQQCV RCCRAFLEKA
bovine	118	SY.DPQKQLI IEDFPYGNDA	DFETVYQQCV RCCRAFLEKV
yeast	116	EXASPGVSKI VDDFPYGGSD	GFGDCTIQLV DFSQNLKSI
human(s)	157	H^	
human(f)	157	H^	
bovine	157	R^	
yeast	156	A^	

FIGURE 1: Sequence alignment of the low M_r PTPases from cyanobacteria (Wilbanks & Glazer, 1993), yeast (Mondesert et al., 1994), bovine (Camici et al., 1989), and human (Dissing et al., 1991). Human(s) and human(f) designate the two human isozymes of the low M_r PTPases. The bold letters indicate invariant residues. The asterisks indicate amino acids in the PTPase signature motif which also correspond to the most conserved region for the low M_r PTPases. The symbol ^ indicates the translation stop.

of the PTP1B and the *Yersinia* PTPase, residues of the PTPase signature motif (12–19 in the low M_r phosphatase, residues 403–410 in the *Yersinia* PTPase, and residues 214–222 in PTP1B) form a similar loop structure termed the phosphate-binding loop between the β -turn at the COOH-terminus of a β -strand and the first turn of an α -helix. These PTPases appear to represent striking examples of convergent evolution. The structural data further support the placement of the low M_r enzymes in the general family of PTPases.

Although extensive mechanistic and structural studies have been carried out on the low M_r PTPases (Zhang & Van Etten, 1991a,b; Wo et al., 1992; Cirri et al., 1993; Su et al., 1994; Zhang, M., et al., 1994), the biological functions of this class of enzymes are not known. Low M_r PTPases were previously known only to exist in mammalian species. The recent genetic studies of fission yeast (*Schizosaccharomyces pombe*) with temperature-sensitive mutations of *cdc25* (i.e., *cdc25-22*) have led to the discovery of a gene that rescues *cdc25-22* when overexpressed (Mondesert et al., 1994). This gene, named *stp1*⁺ (small tyrosine phosphatase), encodes a protein that is highly similar (42% identical) to the mammalian low M_r PTPases. Furthermore, a partial open reading frame (ORF65) in the genome of the cyanobacteria *Synechococcus* sp. WH8020 also encodes a region of sequence identity with the active site of the low M_r PTPases (Wilbanks & Glazer, 1993; and Figure 1). These findings that low M_r PTPases are highly similar in structure among bacteria, yeast, and mammalian species suggest that these enzymes have important biological functions.

Although the yeast *Stp1* share significant sequence similarity with the mammalian low M_r PTPases, it is not known whether *Stp1* can function as a phosphatase. We describe here the expression, purification, and characterization of the recombinant yeast homolog of the mammalian low M_r PTPases, *Stp1*. We demonstrate that *Stp1* possess intrinsic phosphatase activity toward not only aryl but also alkyl phosphates. *Stp1* can also dephosphorylate phosphotyrosine-

containing peptide and protein. We also demonstrate burst kinetics with *Stp1* using *p*-nitrophenyl phosphate as a substrate, suggesting that the rate-limiting step corresponds to the decomposition of the phosphoenzyme intermediate. Surprisingly, we find that the bovine heart low M_r PTPase can dephosphorylate both phosphotyrosyl and phosphoseryl/threonyl protein substrate. Thus, low M_r PTPases likely represent another group of dual specificity phosphatases.

MATERIALS AND METHODS

Materials. *p*-Nitrophenyl phosphate (*p*NPP), β -naphthyl phosphate, *O*-phospho-L-tyrosine, *O*-phospho-L-serine, *O*-phospho-L-threonine, and flavin mononucleotide (FMN; riboflavin 5'-phosphate) were purchased from Sigma. Solutions were prepared using deionized and distilled water. The low molecular weight PTPase from bovine heart was purified to homogeneity as described previously (Zhang & Van Etten, 1990).

Construction of the Expression Plasmids. The polymerase chain reaction (PCR) was used to obtain the cDNA encoding the yeast low molecular weight PTPase, *Stp1*, from the plasmid pBluescript SK that carried a 0.9 kb *Bam*HI–*Sal*I DNA fragment containing *stp1*⁺ cDNA (Mondesert et al., 1994). The PCR primers were 5'-AGCTGGATCCATATGACCAAGAATATTCAAGT and 5'-ACGCGAATTCCTAAGC AATGGATTGAGG for 5' and 3' primer, respectively. The underlined sequence in the 5' primer is an adapter containing the recognition sequences for *Bam*HI and *Nde*I. The underlined sequence in the 3' primer is an *Eco*RI site downstream of the *Stp1* stop codon. The 493-base-pair PCR product was digested with *Bam*HI and *Eco*RI, and the resulting *Bam*HI/*Eco*RI fragment was then directly ligated into pUC118 to generate pUC118-*Stp1*. This construct was verified by restriction digestion and DNA sequencing of the *Stp1* coding region. The coding region of *Stp1* was then removed by *Nde*I and *Eco*RI digestion and subcloned into the plasmid pT7-7 to generate pT7-7-*Stp1* for overexpression.

Expression and Purification of Recombinant *Stp1*. To purify a large quantity of *Stp1*, an overnight culture (10 mL) was grown from a single colony of pT7-7-*Stp1* and was used to inoculate 1 L 2 \times YT (1.6% tryptone, 1% yeast extract, 0.5% NaCl) containing 100 μ g/mL ampicillin. The culture was grown at 37 °C to an optical density of 0.6–0.9 at 600 nm, induced with 0.4 mM isopropyl β -D-thiogalactoside, and grown for an additional 4–5 h at 37 °C. The cells were harvested by centrifugation at 5000 rpm (Sorvall GSA rotor) for 10 min. The resulting pellet was then resuspended in 40 mL of 100 mM acetate, 100 mM NaCl, and 1 mM EDTA, pH 5.1 buffer (buffer A) and lysed by two passages through a French press, maintaining pressures above 1200 psi. The soluble fraction was isolated by centrifuging the lysates at 15 000 rpm (Sorvall SS-34 rotor) for 20 min at 4 °C. The resultant clear supernatant was added to 15 mL of CM Sephadex C-50 equilibrated in buffer A. Binding of the *Stp1* to the cation exchanger was accomplished by gentle shaking at 4 °C for 30 min. The Sephadex resins were then pelleted gently using a clinical centrifuge, and the unbound supernatant was removed. After washing the gel three times with 35 mL of buffer A, the gel was packed into a column. The column was continuously washed with buffer A until the eluent had a zero optical density at 280 nm. The enzyme

was eluted with a 200 mL linear salt gradient from 100 to 500 mM NaCl in 100 mM acetate and 1 mM EDTA, pH 5.1 buffer. The enzyme was purified further by passing the post CM Sephadex pool through a Sephadex G-100 column (2.5 × 110 cm) equilibrated in buffer A. The protein concentration of the fractions was monitored by the absorbance at 280 nm, and the enzyme activity was followed using *p*NPP as a substrate. The absorption extinction coefficient for the homogeneous Stp1 was calculated to be 0.724 at 280 nm for 1 mg/mL Stp1 according to a published procedure (Gill & von Hippel, 1989).

Expression and Mutation of Human MEK1 and ERK1. The human MEK1 (MAP kinase or ERK kinase 1) and ERK1 (extracellular-signal regulated kinase 1) were expressed as GST (glutathione *S*-transferase) fusion proteins in *Escherichia coli* and purified by glutathione-agarose (Sigma) affinity chromatography as previously described (Guan & Dixon, 1991b). The catalytic essential lysine residue (lysine 71) of human ERK1 was mutated to an arginine by oligonucleotide directed mutagenesis method (Promega). The mutant ERK1* was expressed as GST fusion. Recombinant ERK1* was purified and cleaved from GST by thrombin (Sigma) following published methods (Zheng & Guan, 1993).

Mass Spectrometry and Amino Acid Sequencing. Mass determination of the purified recombinant Stp1 was performed by on an API III triple quadrupole mass spectrometer (Perkin-Elmer SCIEX, Thornhill, ON, Canada) equipped with a pneumatically assisted electrospray ionization source. NH₂-terminal amino acid analysis of the purified Stp1 was performed on an ABI 477A gas phase sequencer.

Enzyme Assay. (1) *Small Phosphate Monoester Substrates.* The PTPase activity of Stp1 was usually assayed at 30 °C in a reaction mixture (0.2 mL) containing 10 mM *p*NPP as substrate. Buffers used were as follow: pH 5.0, 100 mM acetate; pH 6.0, 50 mM succinate; and pH 7.0, 50 mM 3,3-dimethylglutarate. All of the buffer systems contained 1 mM EDTA, and the ionic strength of the solutions were kept at 0.15 M using NaCl. The reaction was initiated by addition of enzyme and quenched after 2–3 min by addition of 1 mL of 1 N NaOH. The nonenzymatic hydrolysis of the substrate was corrected by measuring the control without the addition of enzyme. The amount of product *p*-nitrophenol was determined from the absorbance at 405 nm using a molar extinction coefficient of 18 000 M⁻¹ cm⁻¹. One unit of activity is defined as the amount of enzyme that is needed to hydrolyze 1 μmol of *p*NPP/min at 30 °C. Specific activity is defined as the number of enzyme units per milligram protein. For nonchromogenic substrates, enzyme activity was determined by measuring the production of inorganic phosphate (Zhang & Van Etten, 1990). Michaelis–Menten kinetic parameters were determined from a direct fit of the *v* vs [S] data to the Michaelis–Menten equation using the nonlinear regression program GraFit (Erithacus Software).

(2) *Phosphopeptide Substrate.* A three-component buffer consisting of 0.05 M Tris, 0.05 M Bis-Tris, and 0.1 M acetate was used in the following kinetic analyses. This buffer maintains constant ionic strength over its useful pH range (Ellis & Morrison, 1982). All assays were performed at 30 °C. A continuous spectrophotometric assay described previously (Zhang et al., 1993) was employed to follow the dephosphorylation of tyrosine on a MAP kinase (mitogen

activated protein kinase) peptide (MAP_{177–189}, DHTGFLpTEpYVATR). This assay takes advantage of the difference in absorbance at 282 nm between phosphotyrosine and tyrosine and can be utilized to follow the complete time course of the enzyme-catalyzed hydrolysis of phosphotyrosine-containing peptide. The complete time course of the reaction can be fitted to the integrated form of the Michaelis–Menten equation (eq 1) using a nonlinear least-squares algorithm. Values for *k*_{cat} and *k*_{cat}/*K*_m were obtained for Stp1

$$t = p/k_{\text{cat}}E_0 + (K_m/k_{\text{cat}}E_0) \ln[p_{\infty}/(p_{\infty} - p)] \quad (1)$$

using 0.5 mM peptide and 9 μM enzyme, pH 7 and 30 °C. The *k*_{cat}/*K*_m value for the bovine low molecular weight PTPase was determined by varying peptide concentration (0, 0.136, 0.34, and 0.68 mM) and following the initial rate of tyrosine dephosphorylation. The *k*_{cat}/*K*_m value was calculated from the slope of a plot of initial rate and substrate concentration. Because the *K*_m was too high, the *k*_{cat} value could not be determined.

An HPLC method was used to follow the enzyme-catalyzed hydrolysis at both phosphotyrosine and phosphothreonine of DHTGFLpTEpYVATR (Denu et al., 1995). A Vydac C18 (0.21 × 25 cm) column was attached to an Applied Biosystems 130A Separation System HPLC instrument with UV detection set at 220 nm. The peptides were eluted (150 μL/min) over 60 min using a linear gradient of 15–35% B (80% acetonitrile, 20% water, 0.1% trifluoroacetic acid). Solution A was 0.1% trifluoroacetic acid in water. The retention times of -pTEpY- and -pTEY- were 30 and 44 min, respectively. All peaks were resolved and were verified by matrix-assisted laser desorption mass spectrometry analysis and by coelution with the corresponding authentic peptide. To quench the reaction, an equal volume of 1.5 M acetic acid was added to the aliquot before injection of 20 μL of this sample for HPLC separation.

(3) *Protein Substrate.* MBP (myelin basic protein) was phosphorylated by activated ERK1 as described (Zheng & Guan, 1993). MBP (20 μg) was phosphorylated by ERK1 (1 μg) and GST-MEK1 (1 μg) in 20 μL of kinase buffer (18 mM HEPES, pH 7.4, 10 mM magnesium acetate, 50 μM ATP) containing 20 μCi [*γ*-³²P]ATP at 30 °C for 30 min. Purified ERK1* (10 μg) was phosphorylated by GST-MEK1 (2 μg) in 40 μL of kinase buffer containing 40 μCi [*γ*-³²P]-ATP for 30 min at 30 °C. The kinase reaction was terminated by addition of EDTA to 25 mM. The dephosphorylation reaction was performed in 20 μL of solution containing 50 mM imidazole, pH 7.0, and 0.1% 2-mercaptoethanol at 37 °C for 30 min. Substrate of either phosphorylated MBP (0.2 μg) or ERK1* (1 μg) was used in each assay. The reaction was terminated by addition of SDS sample treatment buffer and analyzed by a 15% SDS-PAGE. The samples were transferred to PVDF (Millipore) membrane and followed by autoradiography. Phosphoamino acid analysis was performed using cellulose plates (Kodak) as described (Boyle et al., 1991).

Rapid Kinetics. Pre-steady-state kinetic measurements of the Stp1-catalyzed hydrolysis of *p*NPP were conducted using a Hi-Tech SF-61 stopped-flow spectrophotometer (dead time 2 ms) with an observation cell length of 1.0 cm. Fast reactions at 30 °C were monitored by the increase in absorbance at 410 nm of the *p*-nitrophenolate product. The final substrate *p*NPP concentration was 5 mM (24-fold higher

Table 1: Purification of the Yeast Low Molecular Weight PTPase, Stp1^a

step	protein (mg)	act. (units)	sp act. (units/mg)	yield (%)	purifn (x-fold)
lysate	484	603	1.24	100	1
supernatant	216	525	2.43	87	2
CM	31	373	12.0	62	9.7
G-100	28	358	12.8	59	10.3

^a The purification table gives the typical yield from 2 L of culture as described under Materials and Methods. One unit of activity is defined as the amount of enzyme that is needed to hydrolyze 1 μ mol of *p*-nitrophenyl phosphate/min at 30 °C.

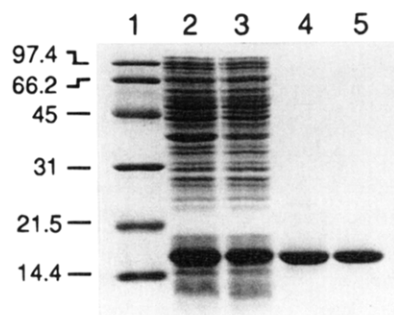


FIGURE 2: SDS-polyacrylamide gel electrophoresis analysis of the purification steps for Stp1. Lane 1, molecular mass standards, from top to bottom: rabbit muscle phosphorylase *b*, 97.4 kDa; bovine serum albumin, 66.2 kDa; hen egg white ovalbumin, 45 kDa; bovine carbonic anhydrase, 31 kDa; soybean trypsin inhibitor, 21.5 kDa; and hen egg white lysozyme, 14.4 kDa. Lane 2, cell lysate. Lane 3, clear cell lysate supernatant. Lane 4, post CM Sephadex C-50. Lane 5, post Sephadex G-100. Protein samples were fractionated on a 15% acrylamide gel and stained with Coomassie Blue.

than the K_m), and the concentration of Stp1 was 71.4 μ M. The extinction coefficient for *p*-nitrophenolate is 1325 M⁻¹ cm⁻¹ at pH 6.0 and 30 °C. The buffer used was 50 mM succinate and 1 mM EDTA, $I = 0.15$ M, pH 6.0. Data collection and analysis were carried out as described previously (Zhang, 1995).

RESULTS AND DISCUSSION

Purification and Physical Characterization. The entire coding sequence of *stp1*⁺ was subcloned behind the bacteriophage T7 promoter in the plasmid pT7-7. High level of expression of Stp1 was obtained by adding isopropyl β -D-thiogalactoside (final concentration 0.4 mM) to the exponentially growing cell culture of *E. coli* BL21 (DE3) carrying the pT7-7-Stp1 plasmid in 2 \times YT media containing 100 μ g/mL ampicillin. The recombinant Stp1 was purified as outlined under Materials and Methods. Table 1 summarizes the overall purification procedure. Almost all the phosphatase activity resided in the clear supernatant of the cell lysate. Greater than 10% of the soluble protein corresponded to Stp1 (Figure 2). The CM Sephadex C-50 cation exchanger was most efficient since Stp1 bound specifically to the resins and most bacteria proteins did not bind at this particular condition. This single step usually yielded almost 95% pure enzyme based on SDS-polyacrylamide gel electrophoresis (lane 4 in Figure 2). Further purification employing a Sephadex G-100 column resulted in a homogeneous preparation of Stp1 (lane 5 in Figure 2). The purified recombinant protein appeared as a single Coomassie Blue staining band after the gel filtration with the anticipated molecular mass of 17 kDa (Figure 2). The homogeneous Stp1 had a specific

Table 2: Comparison of Kinetic Parameters of Yeast Stp1 and Bovine Low M_r PTPase^a

pH	yeast Stp1		bovine heart low M_r PTPase	
	k_{cat} (s ⁻¹)	K_m (mM)	k_{cat} (s ⁻¹)	K_m (mM)
5.0	2.97 \pm 0.26	0.050 \pm 0.005	19.9 \pm 0.3	0.42 \pm 0.03
6.0	3.58 \pm 0.41	0.21 \pm 0.07	19.6 \pm 0.17	0.98 \pm 0.09
7.0	3.48 \pm 0.08	0.37 \pm 0.03	18.0 \pm 0.5	2.11 \pm 0.15

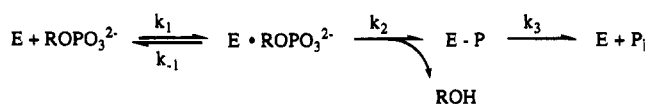
^a All measurements were made at 30 °C, using *p*NPP as a substrate. Buffers used were as follows: pH 5.0, 100 mM acetate; pH 6.0, 50 mM succinate; pH 7.0, 50 mM 3,3-dimethylglutarate. In all the buffer systems, 1 mM EDTA was included, and the ionic strength was kept at 0.15 M, adjusted by NaCl.

activity of 12.8 units/mg at pH 6.0, $I = 0.15$ M, 30 °C, using *p*-nitrophenyl phosphate (*p*NPP) as a substrate. Approximately 28 mg of recombinant Stp1 was obtained from 2 L of culture.

In order to validate the integrity of the enzyme preparation, the purified Stp1 was subjected to amino acid sequence and mass spectrometric analyses. Amino-terminal sequencing up to 10 cycles for Stp1 established that the protein begins with Met-Thr-Lys-Asn-Ile-Gln-Val-Leu-Phe-Val. This is identical to the amino acid sequence predicted by the cDNA sequence (Mondesert et al., 1994). Molecular mass determination of the purified recombinant Stp1 was carried out using electrospray ionization mass spectrometry. The measured molecular mass of the Stp1 is 17391.5 \pm 1.7 Da, which is almost identical to the average molecular mass of 17391.9 Da calculated from the cDNA sequence of the Stp1. Having large quantities of pure Stp1 should facilitate detailed mechanistic and substrate specificity studies of the yeast low M_r PTPase.

Kinetic Properties of Stp1. Although the yeast Stp1 has been shown to share 42% sequence identity with the mammalian low M_r PTPases, it is not known whether Stp1 can function as a phosphatase. With large amounts of homogeneous recombinant yeast Stp1 protein, we proceeded to study its kinetic properties and active site substrate specificity. Since the yeast Stp1 possesses the PTPase signature motif which is identical to that in the mammalian low M_r PTPases (Figure 1), we expect that Stp1 should be an active phosphatase. The enzyme-catalyzed hydrolysis of small phosphate monoesters was followed by either the production of *p*-nitrophenolate (from *p*NPP) or the production of inorganic phosphate as measured by the standard phosphomolybdate colorimetric method (Black & Jones, 1983; Zhang & Van Etten, 1990). All enzyme assays were performed at 30 °C in buffers with a constant ionic strength of 0.15 M containing 1 mM EDTA. We observed that Stp1 possess intrinsic phosphatase activity toward both aryl and alkyl phosphates, phosphotyrosyl peptide, and phosphotyrosyl protein (discussed below). We also purified the bovine heart low M_r PTPase to homogeneity using a procedure described previously (Zhang & Van Etten, 1990). Since the bovine enzyme has been studied extensively (Zhang & Van Etten, 1991a,b), the kinetic characteristics of the yeast enzyme were compared with those of the bovine enzyme. An examination of the pH dependency of the Stp1-catalyzed hydrolysis of *p*NPP showed that, similar to the bovine enzyme, k_{cat} was almost completely flat between pH 5 and pH 7 (Table 2). Interestingly, compared with the bovine enzyme under identical experimental conditions, Stp1 exhibited 6-fold lower k_{cat} and K_m values when *p*NPP was used

Scheme 1



as a substrate.

The low M_r PTPases effect catalysis of phosphate monoester hydrolysis through the formation of a covalent thiophosphate enzyme intermediate involving the active site cysteine residue as a nucleophile (Wo et al., 1992; Cirri et al., 1993). The minimal kinetic scheme for the catalyzed reaction is given in Scheme 1, which is composed of substrate binding, followed by two chemical steps, phosphorylation (k_2) and dephosphorylation (k_3) of the enzyme, where E is the enzyme, ROPO_3^{2-} the substrate, $\text{E} \cdot \text{ROPO}_3^{2-}$ the enzyme-substrate Michaelis complex, $\text{E}-\text{P}$ the phosphoenzyme intermediate, ROH the phenol or alcohol, and P_i inorganic phosphate. For the bovine enzyme, the decomposition of the cysteinyl phosphate enzyme intermediate (k_3) is the rate-limiting step for the overall hydrolysis reaction (Zhang & Van Etten, 1991a), and as a result, it exhibits no dependence on the leaving group $\text{p}K_a$ values (Table 3; Zhang & Van Etten, 1991a,b). Similarly, at pH 6.0 and 30 °C, the k_{cat} values for the yeast Stp1-catalyzed hydrolysis of aryl phosphates such as *p*NPP, β -naphthyl phosphate, and *O*-phospho-L-tyrosine are effectively constant (Table 3). The leaving group $\text{p}K_a$ values are 7.14, 9.38, and 10.07 for *p*-nitrophenol, β -naphthol, and tyrosine (Zhang & Van Etten, 1991b). Thus, it is likely that the rate of the reaction catalyzed by Stp1 is also determined by the breakdown of the phosphoenzyme intermediate. Flavin mononucleotide (FMN) was identified as a likely biological substrate for the low M_r PTPases (Heinrikson, 1969). We were struck by the observation that Stp1 brought about the hydrolysis of FMN with a k_{cat} value that is identical to those of aryl phosphates. A similar result was obtained with the bovine enzyme (Table 3). Since FMN is an alkyl phosphate, this appears contradictory to the low M_r PTPase's high specificity toward aryl phosphates (Zhang & Van Etten, 1990). Although only 70% of the commercial preparation corresponds to authentic FMN, a careful study established that indeed the bovine low M_r PTPase had intrinsic phosphoesterase activity toward FMN (Zhang & Van Etten, 1990). The fact that the low M_r PTPases show high activity toward FMN and are inactive against most alkyl phosphates examined suggests that there may be a hydrophobic binding pocket at or near the enzyme active site which is specific for the aromatic moiety of the substrate, because electrostatic interaction between the phosphate group and the enzyme active site cannot by itself explain the distinctive reactivity of FMN. Consistent with this, alkyl phosphate monoesters having a pendant aromatic group ($\text{Ph}(\text{CH}_2)_n\text{OPO}_3\text{H}_2$, $n = 1-5$) are all fairly good substrates (Zhang & Van Etten, 1991b). The three-dimensional structure of the bovine heart low M_r PTPase shows that the active site is relatively exposed to the solvent (Zhang, M., et al., 1994). Along the sides of the catalytic cleft are side chains of one tryptophan (Trp49) and two tyrosines (Tyr131 and Tyr132) that extend out like two claws on a lobster. These residues are also conserved in the yeast enzyme (Figure 1). This arrangement of the two types of aromatic residues on the surface of the molecule contributes to a large hydrophobic patch near the active site, which may be important in determining substrate specificity.

The yeast Stp1 and the bovine low M_r PTPase both catalyze the hydrolysis of *O*-phospho-L-serine, with k_{cat} values that are 70- and 220-fold slower than those of the aryl phosphates (Table 3). *O*-Phospho-L-threonine is inert toward the yeast and bovine enzymes. This likely arises from the sensitivity of the nucleophilic displacement reaction to steric hindrance, since *O*-phospho-L-threonine is the alkyl phosphate of a secondary alcohol. The hydrolysis of both aryl and alkyl phosphates can be effectively blocked by the presence of 1 mM vanadate, a good competitive inhibitor of the low M_r PTPases (Zhang & Van Etten, 1990). This suggests that the low M_r phosphatases catalyze the hydrolysis of aryl and alkyl phosphates *via* the same active site. Thus, it appears that the low M_r PTPases possess intrinsic phosphatase activity toward alkyl phosphates.

Burst Kinetics. Our leaving group dependence data (Table 3) suggest that Stp1-catalyzed hydrolysis of phosphate monoesters is rate-limited by the decomposition of the phosphoenzyme intermediate. To provide direct kinetic evidence for this, we turned to pre-steady-state stopped-flow spectroscopic techniques with Stp1 using *p*NPP as a substrate. The analysis of burst kinetics for PTPase-catalyzed hydrolysis has been described previously (Zhang & Van Etten, 1991a; Zhang, 1995). Briefly, when $[\text{S}] \gg [\text{E}]$, the increase in *p*-nitrophenolate concentration as a function of time can be described as $[\text{p-nitrophenolate}] = At + B(1 - e^{-bt})$. The individual rate constants for the enzyme phosphorylation (k_2) and dephosphorylation (k_3) can be determined from the exponential ($b = k_2 + k_3$) and the linear phase ($A = k_2k_3/(k_2 + k_3)$), respectively (Scheme 1). The size of the burst $B = E_0[k_2/(k_2 + k_3)]^2/(1 + K_m/S_0)^2$ and is proportional to the active enzyme concentration. So if k_2 and k_3 are comparable, one should observe a "burst" of *p*-nitrophenol production using *p*NPP as a substrate. At 4.5 °C and pH 7, burst kinetics has been demonstrated with the bovine enzyme (Zhang & Van Etten, 1991a). It is not known whether similar burst kinetic phenomena can be observed at more physiological temperatures. There is always a possibility that changing reaction temperature may alter the ratio of k_2 and k_3 and lead to a change in the rate-limiting step of the enzyme-catalyzed reaction. The phosphorylation (k_2) and dephosphorylation (k_3) rate constants for the bovine enzyme have been estimated by steady-state partition experiments to be 540–790 s^{-1} and 31–36 s^{-1} , respectively, at 37 °C (Zhang & Van Etten, 1991a; Taddei et al., 1994). The rate constant for the intermediate formation (k_2) is at the detection limit of a stopped-flow spectrophotometer, which makes direct observation of the burst for the mammalian enzyme technically more difficult. The yeast enzyme is 6-fold slower than the mammalian enzyme and may represent a good model for rapid kinetic studies of the low M_r PTPases.

We performed a pre-steady-state stopped-flow kinetic analysis of the Stp1-catalyzed hydrolysis of *p*NPP at pH 6.0 and 30 °C. When the reaction was monitored at 410 nm to detect the *p*-nitrophenolate ion product, the absorbance time course was biphasic, characterized by a rapid, exponential phase which is then followed by a slower linear phase (Figure 3). By varying the initial concentration of the enzyme and the substrate, we found that the amplitude of the burst is proportional to the enzyme concentration and that the dependency of the burst size on the substrate concentration can be adequately described by $B = E_0[k_2/(k_2 + k_3)]^2/(1 + K_m/S_0)^2$. For example, the experimentally determined burst

Table 3: Kinetic Parameters for Various Aryl and Alkyl Phosphates at pH 6.0

substrate	pK_a of leaving group	yeast Stp1		bovine heart low M_r PTPase	
		k_{cat} (s^{-1})	K_m (mM)	k_{cat} (s^{-1})	K_m (mM)
<i>p</i> -nitrophenyl phosphate	7.14	3.58 ± 0.41	0.21 ± 0.07	19.6 ± 0.17	0.98 ± 0.09
β -naphthyl phosphate	9.38	2.97 ± 0.04	0.19 ± 0.01	18.3 ± 0.57	1.67 ± 0.15
<i>O</i> -phospho-L-tyrosine	10.07	3.09 ± 0.09	1.50 ± 0.14	19.1 ± 0.81	16.1 ± 3.5
flavin mononucleotide	13–15	3.62 ± 0.11	1.09 ± 0.11	17.1 ± 3.8	6.50 ± 1.8
<i>O</i> -phospho-L-serine	13–15	0.046 ± 0.002	24.7 ± 1.7	0.086 ± 0.014	17.3 ± 2.2
<i>O</i> -phospho-L-threonine	13–15	ND	ND	ND	ND

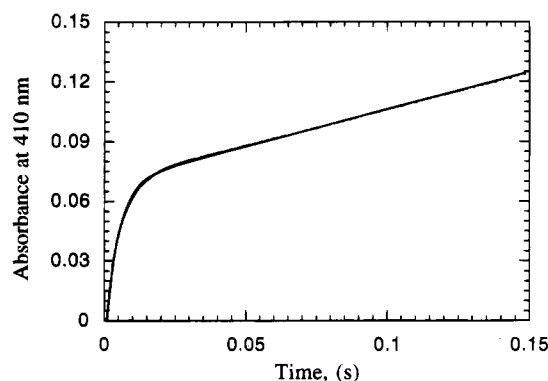
^a ND, not detectable.

FIGURE 3: Burst kinetics observed with yeast Stp1 and *p*NPP at pH 6 and 30 °C. The Stp1 concentration was 71.4 μ M. The *p*NPP concentration was 5 mM. Each stopped-flow trace was an average of at least 6 individual experiments. The solid line represents a theoretical fit of the data to the equation $[p\text{-nitrophenolate}] = At + B(1 - e^{-bt}) + C$.

for Stp1 (71.4 μ M) at pH 6.0 and 5 mM *p*NPP (Figure 3) was 64.3 μ M and corresponded to 90% of the enzyme concentration. The steady-state kinetic parameters (determined independently of the stopped-flow experiments) at 30 °C and pH 6.0 for Stp1 using *p*NPP as a substrate were $k_{cat} = 3.58 \text{ s}^{-1}$ and $K_m = 0.21 \text{ mM}$. The individual rate constant for the intermediate formation (k_2) and breakdown (k_3) was calculated to be 161 s^{-1} and 4 s^{-1} , respectively, from the relationships: $b = k_2 + k_3 = 165 \text{ s}^{-1}$ and $A = k_2k_3/(k_2 + k_3) = 3.88 \text{ s}^{-1}$. Thus, the rate for the intermediate formation is 40-fold faster than the rate of the intermediate decomposition. The maximal theoretical burst calculated from these values is 62.6 μ M, which corresponds to 88% of the enzyme active site concentration at a substrate concentration of 5 mM. Thus there is good agreement between the directly observed amplitude of the burst with the theoretically predicted value based on the specific experimental conditions. Overall, these results establish that the rate-limiting step of the Stp1-catalyzed hydrolysis of phosphate monoesters is k_3 , the decomposition of the phosphoenzyme intermediate.

Demonstration of burst kinetics with Stp1 provides direct kinetic evidence for the involvement of a phosphoenzyme intermediate in Stp1 catalysis. It also enables us to determine the individual rate constants directly associated with the formation (k_2) and breakdown (k_3) of the phosphoenzyme intermediate. More importantly, this approach combined with the technique of site-directed mutagenesis should allow one to ascertain specific contributions of active site amino acid side chains to the individual steps of the low M_r PTPase-catalyzed reaction. For example, the crystal structures of the bovine low M_r PTPase have implicated an aspartic acid, Asp129, on a loop adjacent to the phosphate-binding loop as a potential general acid in catalysis (Su et al., 1994; Zhang,

M., et al., 1994). Recent mutational studies provided evidence for the importance of Asp129 in catalysis, but the detailed mechanism and the specific step(s) that is effected by Asp129 remained controversial due to the inherent limitations of steady-state kinetics (Taddei et al., 1994; Zhang, Z., et al., 1994). Detailed pre-steady-state kinetic analysis of the corresponding mutants of Asp128 in the yeast enzyme should lead to a better understanding of the role of this critical aspartic acid in catalysis.

Substrate Specificity of the Low M_r PTPases. It has been previously shown that the bovine low M_r PTPase can hydrolyze phosphotyrosine residues in several peptides and proteins (Chernoff & Li, 1985; Waheed et al., 1988; Ramponi et al., 1989). Because the yeast low M_r PTPase, Stp1, can rescue the function of the cell cycle regulator *cdc25*, a dual specificity phosphatase, we wished to explore further the substrate specificity of the low M_r PTPases. We have already shown that both the yeast and the bovine enzymes exhibited intrinsic phosphatase activity toward phosphoserine. We then tested the Thr/Ser phosphorylated MBP and the Tyr/Thr phosphorylated ERK1* as substrates for both the bovine and yeast low M_r PTPases. The phosphorylated protein substrate preparations and phosphatase activity assays were described under Materials and Methods. Our results demonstrated that both enzymes could dephosphorylate tyrosine residues of the Tyr/Thr phosphorylated ERK1* (lanes 4–6, Figure 4). Because the Thr phosphorylation level in ERK* was very low, we could not completely rule out the possibility that dephosphorylation occurred on the Thr residue in the presence of the low M_r PTPases. When Thr/Ser phosphorylated MBP was used as a substrate, dephosphorylation was observed only with the bovine enzyme (lane 2, Figure 4) but not with the yeast PTPase (lane 3, Figure 4). The bovine PTPase hydrolyzed both phosphothreonine and phosphoserine residues of MBP (lane 2, Figure 4C). Given the qualitative nature of the data, it does not appear that the activity of bovine low M_r PTPase toward the phosphotyrosyl ERK* differs greatly from its activity toward the phosphoseryl/threonyl MBP (Figure 4). The lack of dephosphorylation of Thr/Ser phosphorylated MBP by the yeast low M_r PTPase is not due to insufficient phosphatase used in the assay because identical amount of this enzyme dephosphorylated ERK1* more effectively than the bovine PTPase (lanes 4–6, Figure 4). The yeast enzyme did not dephosphorylate the phosphoserine in MBP even when a higher concentration of the substrate was used in the assay (data not shown). It is noteworthy that an early study also indicated that the bovine heart low M_r PTPase had serine/threonine phosphatase activity toward phosphoseryl phosphorylase *a* and phosphoseryl casein (Chernoff & Li, 1985). Although that work was carried out with a less than

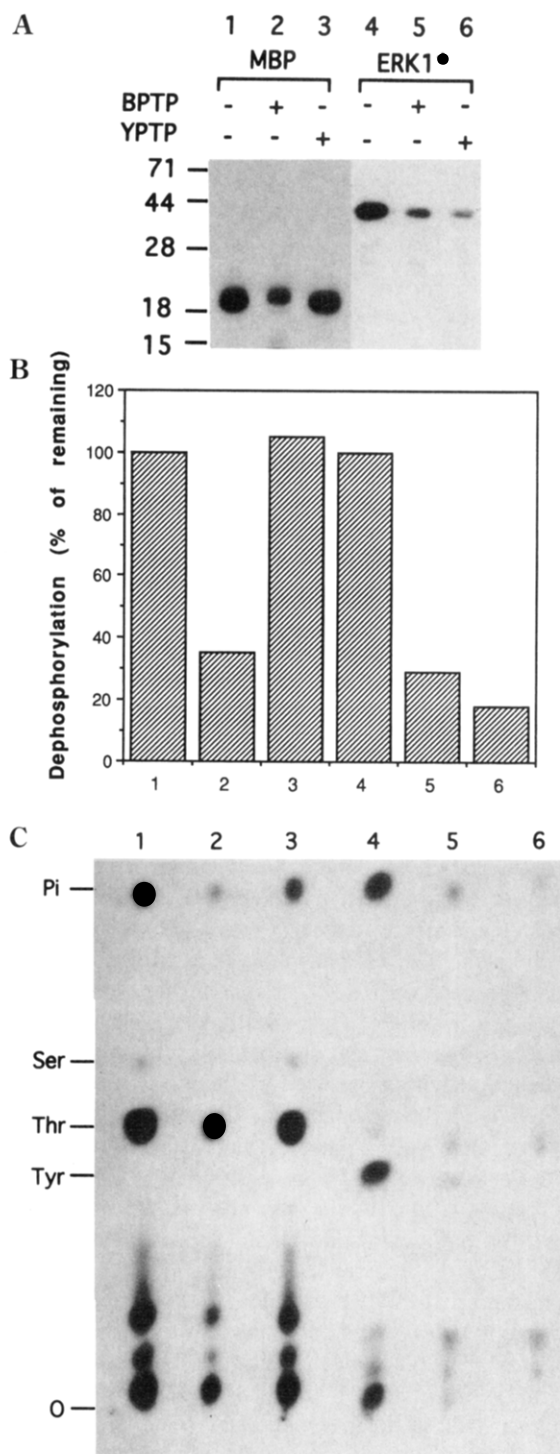


FIGURE 4: Dephosphorylation of MBP and ERK1*. (A) Dephosphorylation of MBP and ERK1* analyzed by SDS-PAGE. Phosphorylated MBP (0.2 μ g) was dephosphorylated by the bovine low M_r PTPase (BPTP, 2.5 μ g, lane 2) or yeast low M_r PTPase (YPTP, 2.5 μ g, lane 3). Lane 1 indicates the untreated MBP as a control. Autoradiograph was exposed for 45 min for lanes 1–3. Phosphorylated ERK1* (lane 4, 1 μ g) was treated with the bovine low M_r PTPase (BPTP, 2.5 μ g, lane 5) or the yeast low M_r PTPase (YPTP, 2.5 μ g, lane 6). The film was exposed for 4 h for lanes 4–6. Molecular weight standards are indicated on the left. (B) Quantitation of dephosphorylation. The radioactivity of 32 -P of MBP and ERK1* after dephosphorylation was quantitated by phosphorimage and compared to those in panel A. Lanes 1–6 are identical to those in panel A. (C) Phosphoamino acid analysis. The protein bands corresponding to panel A were excised and subjected to phosphoamino acid analysis. Pi, Ser, Thr, Tyr, and O denote the positions of free phosphate, phosphoserine, phosphothreonine, phosphotyrosine, and origin, respectively. Lanes 1–6 are identical to those in panel A.

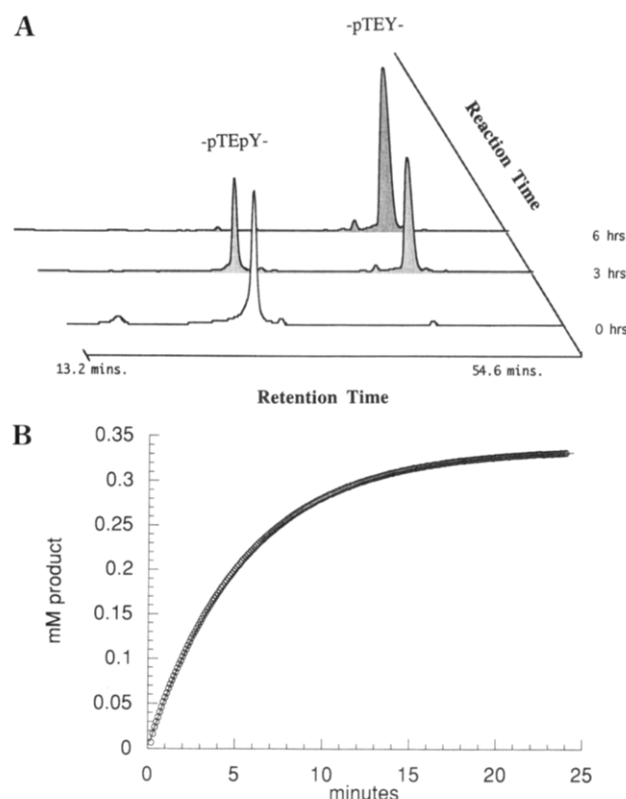


FIGURE 5: (A) HPLC elution profile of the bovine low M_r PTPase-catalyzed hydrolysis of the diphosphorylated MAP_{177–189} kinase peptide (DHTGFLpTEpYVATR). The reactions were performed at pH 7 and 30 °C. The initial peptide concentration was 500 μ M, and the enzyme concentration was 3.6 μ M. The retention times of -pTEpY- and -pTEY- were 30 and 44 min, respectively. (B) Time course of the Stp1-catalyzed hydrolysis of the phosphotyrosine residue in the diphosphorylated MAP_{177–189} kinase peptide (DHTGFLpTEpYVATR) at pH 7 and 30 °C. The peptide substrate concentration was 500 μ M, and the enzyme concentration was 9 μ M. The theoretical curve (solid line) was obtained through a nonlinear least-squares fit algorithm to the experimental data using the integrated Michaelis–Menten equation.

homogeneous preparation of the bovine enzyme, it agrees with our current results using homogeneous enzyme.

In order to obtain kinetic parameters for the dual specificity of the low M_r PTPases, we employed the stoichiometrically diphosphorylated MAP kinase peptide (MAP_{177–189}, DHTGFLpTEpYVATR) as a substrate. The activation of MAP kinases require the phosphorylation of both the Thr and the Tyr residues in the -T₁₈₃EY₁₈₅- motif. All of the assays were done at pH 7 and 30 °C. An HPLC method was used to monitor all possible dephosphorylations of DHTGFLpTEpYVATR within a single experiment. This method is based on the fact that the retention times of the diphosphorylated peptide in the various phosphorylation states were different. Using the dual-specific phosphatase VHR, this method was successfully employed to determine the rates of both tyrosine and threonine dephosphorylation on this peptide (Denu et al., 1995). Figure 5A shows the elution profile at different reaction times of the hydrolysis of the diphosphorylated peptide DHTGFLpTEpYVATR catalyzed by the bovine low M_r PTPases. We only observed dephosphorylation on the tyrosine residue for both the yeast and bovine enzymes. There was no discernible hydrolysis on the phosphothreonine residue. The retention times of -pTEpY- and -pTEY- were 30 and 44 min, respectively. All peaks were resolved and were verified by matrix-assisted laser desorption mass

spectrometry analysis and by coelution with the corresponding authentic peptide. It is interesting that although we have shown that the bovine enzyme is capable of removing phosphate from both serine and threonine residues in MBP, it could not dephosphorylate the threonine residue in either ERK* or peptide DHTGFLpTEpYVATR even after prolonged incubation with high enzyme concentration. This suggests that the low M_r PTPases may have rather stringent substrate specificity.

A continuous spectrophotometric assay described previously (Zhang et al., 1993) was then used to follow the dephosphorylation of tyrosine on MAP kinase peptide DHTGFLpTEpYVATR. This assay takes advantage of the difference in absorbance at 282 nm between phosphotyrosine and tyrosine and can be utilized to follow the complete time course of the enzyme-catalyzed hydrolysis of phosphotyrosine-containing peptide (Figure 5B). The complete time course of the reaction can be fitted to the integrated form of the Michaelis–Menten equation (see Materials and Methods) using a nonlinear least-squares algorithm. Values of k_{cat} and k_{cat}/K_m for the yeast enzyme were $0.38 \pm 0.02 \text{ s}^{-1}$ and $416 \pm 2 \text{ M}^{-1} \text{ s}^{-1}$, respectively. The k_{cat}/K_m value for the bovine low M_r PTPase was determined by varying peptide concentration (0, 0.136, 0.34, and 0.68 mM) and following the initial rate of tyrosine dephosphorylation. The k_{cat}/K_m value was calculated as $23.6 \pm 1.2 \text{ M}^{-1} \text{ s}^{-1}$ from the slope of a plot of initial rate and substrate concentration. Because the K_m was too high, the k_{cat} value could not be determined.

The Low M_r PTPases Are Dual Specificity Phosphatases. In this paper we have shown that both the yeast and the bovine heart low M_r PTPases possess intrinsic phosphatase activity toward alkyl phosphates such as FMN and *O*-phospho-L-serine. In addition, we have demonstrated that both the yeast and the bovine enzymes can also bring about dephosphorylation of tyrosine residues in peptide and protein substrates. More importantly, we have also demonstrated that the bovine low M_r PTPase can carry out hydrolysis of both phosphothreonine and phosphoserine residues of MBP. We therefore suggest that the bovine heart low M_r PTPase should be classified as a dual specificity phosphatase. Dual specificity phosphatases are enzymes that are capable of removing phosphate from both phosphotyrosine and phosphoserine/threonine-containing proteins (Guan et al., 1991). Both enzymes showed low protein phosphatase activities, which may be due either to the enzyme's high substrate selectivity or the artificial substrates being not the best substrates.

Recently, it has become apparent that there exists a large group of dual specificity phosphatases which includes the *Vaccinia* phosphatase, VH1 (for *Vaccinia* open reading frame H1; Guan et al., 1991), the cell cycle regulator Cdc25 (Millar & Russell, 1992), and a number of mammalian dual specificity phosphatases which are capable of dephosphorylating and inactivating MAP kinase (Sun et al., 1993; Ward et al., 1994). The dual specificity phosphatases also possess the PTPase signature motif (H/V)C(X)₅R(S/T) but otherwise display little amino acid sequence identity with the PTPases. On the basis of amino acid sequence comparison, it has been proposed that the dual specificity phosphatases can be further divided into VH1 and its eukaryotic homologs, the baculovirus phosphatase (BVP) and its homologs, and the Cdc25 homologs (Sheng & Charbonneau, 1993). Our results place the low M_r PTPases as another group of the dual specificity

phosphatases. These dual specificity phosphatase subfamilies may have diverged from one another in order to perform specialized functions requiring the recognition of specific substrates or responsiveness to a particular mode of regulation (Sheng & Charbonneau, 1993). A striking characteristic of the dual specificity phosphatases is their high specificity toward substrate. For example, the cell cycle regulator, Cdc25, has been shown to operate only on its physiological substrate, the cyclin-dependent protein kinase Cdc2 (Gautier et al., 1991). The immediate early gene 3CH134 encodes a dual specificity phosphatase that inactivates MAP kinase *in vivo* by direct dephosphorylation of the critical residues Thr183 and Tyr185 (Sun et al., 1993). Although 3CH134 hydrolyzes a variety of phosphotyrosyl peptides/proteins, it does not dephosphorylate phosphoseryl/threonyl peptides/proteins *in vitro* (Charles et al., 1993). The relative high selectivities and varied kinetic properties of the dual specificity phosphatases toward model substrates suggest that there may be additional sites of interactions between the phosphatases and the protein substrates that may be important for effective catalysis.

The low M_r PTPases have been studied for decades. The *in vivo* functions of the mammalian enzymes are unknown. The finding that low M_r PTPases are highly similar in structure from bacteria, yeast, and mammalian species suggests these enzymes play important roles. The yeast low M_r PTPase, Stp1, was found to complement Cdc25 (Mondesert et al., 1994). In fission yeast, Cdc25 protein phosphatase dephosphorylates Tyr15 of Cdc2, thereby activating Cdc2/cyclin B kinase, which then brings about mitosis (Millar & Russell, 1992; Norbury & Nurse, 1992). Phosphorylation of Thr14 in Cdc2 of fission yeast has not been observed. This is consistent with the tyrosine phosphatase activity of Stp1 demonstrated in this study. In animal cells, however, dephosphorylation of Tyr15 in Cdc2 is not sufficient to activate the kinase. The Cdc2 kinase activity in animal cells is maintained in an inactive state by phosphorylation on not only Tyr15 but also the adjacent Thr14 residue. Dephosphorylation of both Tyr15 and Thr14 residues is mediated by animal proteins homologous to Cdc25, which may have a general role in determining the timing of the onset of mitosis in postembryonic animal cell cycles (Millar & Russell, 1992; Norbury & Nurse, 1992). In light of the fact that Stp1 can rescue Cdc25 temperature-sensitive mutations in fission yeast, indicating that Stp1 can dephosphorylate Cdc2 *in vivo*, it is possible that the mammalian low M_r PTPases play an important role in cell cycle control. That the bovine low M_r PTPase displays phosphatase activity against both phosphotyrosine and phosphoserine/threonine is consistent with this proposal, although this needs to be proven experimentally. The molecular feature that is responsible for the difference in substrate specificity between the yeast and mammalian low M_r PTPases is not known. The yeast Stp1 may or may not have phosphatase activity toward phosphoseryl/threonyl protein substrates *in vivo*, since we have only looked at two artificial substrates. More systematic investigation of the molecular recognition between the yeast low M_r PTPase and its substrates should help to resolve this issue. With homogeneous preparations of both enzymes, further detailed comparative substrate specificity studies should be possible.

Conclusion. In this study we described a simple, efficient procedure for obtaining large quantities of the yeast low M_r

PTPase, Stp1. We showed that Stp1 is an active phosphatase hydrolyzing both aryl and alkyl phosphates. Stp1 was also able to dephosphorylate phosphotyrosyl peptide and protein. The availability of large amounts of enzyme has also resulted in a pre-steady-state kinetic analysis of the Stp1-catalyzed reaction. We demonstrated that the Stp1-catalyzed hydrolysis of pNPP is rate-limited by the decomposition of the phosphoenzyme intermediate. Since the turnover number for the Stp1-catalyzed reaction is 6 times slower than that of the mammalian low M_r PTPases, the yeast enzyme is a good model for detailed rapid kinetic studies in order to define the function of essential active site residues in catalysis. Finally, we also demonstrated that the bovine heart low M_r PTPase was capable of dephosphorylating both phosphotyrosyl and phosphoserine/threonine protein substrates. The substrate specificity and recognition of the low M_r PTPases is restricted and may be primarily determined by the amino acid sequence surrounding the phosphorylation site and the overall three-dimensional conformation of the substrate molecule. We suggest that the low M_r PTPases, like Cdc25 family of phosphatases, may represent a new group of dual specificity phosphatases which may be involved in cell cycle control.

ACKNOWLEDGMENT

We thank Dr. John Blanchard for the use of the stopped-flow instrument. Protein sequencing was performed in the Laboratory of Macromolecular Analysis of AECOM.

REFERENCES

- Barford, D., Flint, A. J., & Tonks, N. K. (1994) *Science* 263, 1397–1404.
- Black, M. J., & Jones, M. E. (1983) *Anal. Biochem.* 135, 233–238.
- Boyle, W. J., van de Geer, P., & Hunter, T. (1991) *Methods Enzymol.* 201, 508–519.
- Camici, G., Manao, G., Cappugi, G., Modesti, A., Stefani, M., & Ramponi, G. (1989) *J. Biol. Chem.* 264, 2560–2567.
- Charles, C. H., Sun, H., Lau, L. F., & Tonks, N. K. (1993) *Proc. Natl. Acad. Sci. U.S.A.* 90, 5292–5296.
- Chen, C.-H., & Chen, S. C. (1988) *Arch. Biochem. Biophys.* 262, 427–438.
- Chernoff, J., & Li, H. C. (1985) *Arch. Biochem. Biophys.* 240, 135–145.
- Cho, H., Krishnaraj, R., Kitas, E., Bannwarth, W., Walsh, C. T., & Anderson, K. S. (1992) *J. Am. Chem. Soc.* 114, 7296–7298.
- Cirri, P., Chiarugi, P., Camici, G., Manao, G., Raugei, G., Cappugi, G., & Ramponi, G. (1993) *Eur. J. Biochem.* 214, 647–657.
- Denu, J. M., Zhou, G., Wu, L., Zhao, R., Yuvaniyama, J., Saper, M. A., & Dixon, J. E. (1995) *J. Biol. Chem.* 270, 3796–3803.
- Dissing, J., Johnsen, A. H., & Sensabaugh, G. F. (1991) *J. Biol. Chem.* 266, 20619–20625.
- Ellis, K. J., & Morrison, J. F. (1982) *Methods Enzymol.* 87, 405–426.
- Gautier, J., Solomon, M. J., Booher, R. N., Bazan, J. F., & Kirschner, M. W. (1991) *Cell* 67, 197–211.
- Gill, S. C., & von Hippel, P. H. (1989) *Anal. Biochem.* 182, 319–326.
- Guan, K. L., & Dixon, J. E. (1991a) *J. Biol. Chem.* 266, 17026–17030.
- Guan, K. L., & Dixon, J. E. (1991b) *Anal. Biochem.* 192, 262–267.
- Guan, K. L., Broyles, S. S., & Dixon, J. E. (1991) *Nature* 350, 359–362.
- Heinrikson, R. L. (1969) *J. Biol. Chem.* 244, 299–307.
- Millar, J. B. A., & Russell, P. (1992) *Cell* 68, 407–410.
- Mondesert, O., Moreno, S., & Russell, P. (1994) *J. Biol. Chem.* 269, 27996–27999.
- Norbury, C., & Nurse, P. (1992) *Annu. Rev. Biochem.* 61, 441–470.
- Ramponi, G. (1994) *Adv. Protein Phosphatases* 8, 1–25.
- Ramponi, G., Manao, G., Camici, G., Cappugi, G., Ruggiero, M., & Bottaro, D. P. (1989) *FEBS Lett.* 250, 469–473.
- Sheng, Z., & Charbonneau, H. (1993) *J. Biol. Chem.* 268, 4728–4733.
- Stuckey, J. A., Fauman, E. B., Schubert, H. L., Zhang, Z.-Y., Dixon, J. E., & Saper, M. A. (1994) *Nature* 370, 571–575.
- Su, X.-D., Taddei, N., Stefani, M., Ramponi, G., & Nordlund, P. (1994) *Nature* 370, 575–578.
- Sun, H., Charles, C. H., Lau, L. F., & Tonks, N. K. (1993) *Cell* 75, 487–493.
- Taddei, N., Chiarugi, P., Cirri, P., Fiaschi, T., Stefani, M., Camici, G., Giovanni, R., & Ramponi, G. (1994) *FEBS Lett.* 350, 328–332.
- Waheed, A., Laidler, P. M., Wo, Y.-Y. P., & Van Etten, R. L. (1988) *Biochemistry* 27, 4265–4273.
- Ward, Y., Gupta, S., Jensen, P., Wartmann, M., Davis, R. J., & Kelly, K. (1994) *Nature* 367, 651–654.
- Wilbanks, S. M., & Glazer, A. N. (1993) *J. Biol. Chem.* 268, 1226–1235.
- Wo, Y.-Y. P., Zhou, M.-M., Stevis, P., Davis, J. P., Zhang, Z.-Y., & Van Etten, R. L. (1992) *Biochemistry* 31, 1712–1721.
- Zhang, M., Van Etten, R. L., & Stauffacher, C. V. (1994) *Biochemistry* 33, 11097–11105.
- Zhang, Z., Harms, E., & Van Etten, R. L. (1994) *J. Biol. Chem.* 269, 25947–25950.
- Zhang, Z.-Y. (1995) *J. Biol. Chem.* 270, 11199–11204.
- Zhang, Z.-Y., & Van Etten, R. L. (1990) *Arch. Biochem. Biophys.* 282, 39–49.
- Zhang, Z.-Y., & Van Etten, R. L. (1991a) *J. Biol. Chem.* 266, 1516–1525.
- Zhang, Z.-Y., & Van Etten, R. L. (1991b) *Biochemistry* 30, 8954–8959.
- Zhang, Z.-Y., & Dixon, J. E. (1994) *Adv. Enzymol.* 68, 1–36.
- Zhang, Z.-Y., Thieme-Sefler, A. M., Maclean, D., Roeske, R., & Dixon, J. E. (1993) *Anal. Biochem.* 211, 7–15.
- Zhang, Z.-Y., Wang, Y., Wu, L., Fauman, E., Stuckey, J. A., Schubert, H. L., Saper, M. A., & Dixon, J. E. (1994) *Biochemistry* 33, 15266–15270.
- Zheng, C. F., & Guan, K. L. (1993) *J. Biol. Chem.* 268, 11435–11439.

BI950886X